VI International Conference on Computational Methods in Marine Engineering
MARINE 2015
F. Salvatore, R. Broglia and R. Muscari (Eds)

EFFECT OF A NEGATIVE STIFFNESS MECHANISM ON THE PERFORMANCE OF THE WEPTOS ROTORS

S. PERETTA[*], P. RUOL[*], L. MARTINELLI[*], A. TETU[‡] AND J. P. KOFOED[‡]

[*] Department of Civil, Environmental and Architectural Engineering (ICEA)
Padova University
Via Ognissanti, 39, 35126 Padova, Italy
e-mail: piero.ruol@unipd.it, www.unipd.it

[‡] Department of Civil Engineering
Aalborg University
Sofiendalsvej 11, Room 11-205
9200 Aalborg SV, Denmark
email: jpk@civil.aau.dk, www.aau.dk

Key words: Negative stiffness, Wave Energy Converter, WEPTOS

Abstract. The WEPTOS is a well-known wave energy converter (www.weptos.com), formed by several rotors, with a shape that draws upon the reputable Salters Duck geometry. The WEPTOS has a large efficiency under waves of one particular frequency, i.e. when resonance conditions occur. In order to extend the range of resonance conditions, the possible use of a negative stiffness in the rotor system is analysed. This note presents some considerations on the effectiveness of negative stiffness based on physical model experiments and on the numerical simulations used to interpret the test results. More specifically, the aim of the work is to evaluate how the WEPTOS performance is affected by the presence of a spring into the system that enhances the rotor oscillations applying a negative (un-stabilizing) torque proportional to the degree of rotation.

Experiments were carried out in the deepwater wave basin of Aalborg University, on a 1:30 scale model of one rotor of the WEPTOS. Three different configurations were analysed, providing different values of the negative stiffness. A set of 16 regular and 5 irregular wave conditions were tested, with maximum heights up to approximately 6 m at prototype scale, periods ranging from 5 to 9 s. The incident wave characteristics, the device rotations and the power dissipated by a dummy power converter were accurately measured. The effect of the negative stiffness was partly hindered by the presence of friction, so that no conclusive evidence could be drawn.

A simple numerical model, where the rotor was interpreted as an oscillating mass-damper-spring system, was set up and calibrated to the experimental results. Reasonably good agreement between predictions and measurements were found at model scale. The numerical simulations at prototype dimensions, where friction effects have a relatively lower importance, revealed that the springs responsible of the negative stiffness increase in fact the efficiency of the device.

1 INTRODUCTION

The performance of wave energy converters should be evaluated from a global point of view, i.e. an approach that includes both the hydraulic response and the generator control (López et al., 2013). In fact, cost benefit analysis (e.g. Azzellino et al, 2011) show that there is a significant potential for economic installations, but the power take off system (PTO) is a critical issue.

The Authors recently focused on experiments that include the actual PTO, the generator response and the operational strategy (Martinelli et al, 2014). Martinelli et al (2013) show a simplified method to anticipate the actual production already after the initial experimental stage, when the PTO is merely substituted by a dummy dissipator. Experiments should be based on the simulation of the real irregular wave climate (e.g. Vicinanza et al, 2013 or Martinelli et al. 2011 for the Mediterranean Sea) and an accurate reproduction of the model to be analyzed, that for this note is the WEPTOS (Pecher et al 2012; 2012b; Ferri et al 2014).

The WEPTOS is a floating structure, composed of two legs hinged at the front, which support 20 rotors having a shape that resembles that of a Salter's duck (Salter, 1974). The rotors connected to the same leg drive a common axle, connected to a PTO system located in the front or middle compartment. The angle formed by the legs is adjustable between 30° and 120° (Figure 2, right) so that the rotor oscillations are not in phase, which leads to a smoothening of the power on the axles. The adaptability of the shape also means that the device can decrease its width relatively to the incoming wave front in order to significantly reduce the forces on the structure under large waves or, conversely, increase the width under operational wave conditions to harvest more wave energy under lower wave conditions.

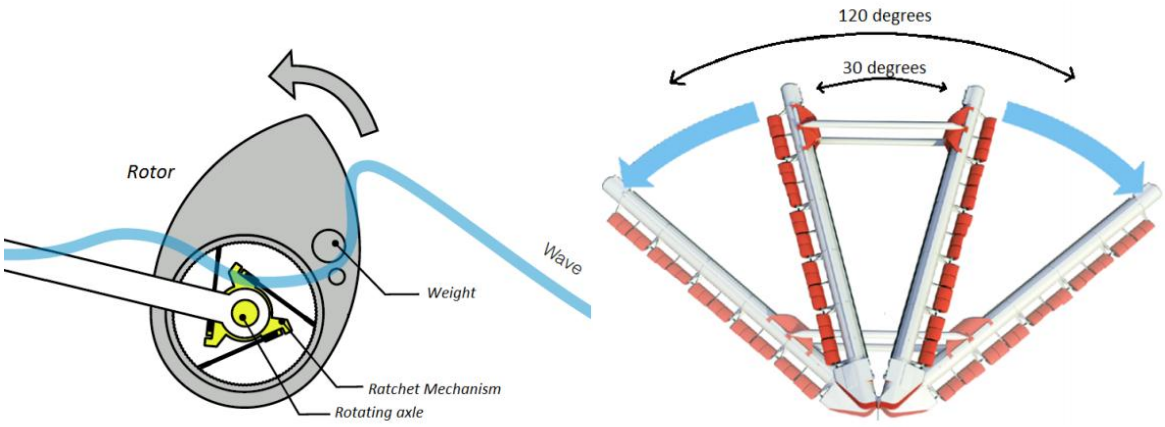

Figure 1: Single rotor (left) ; WEPTOS layout (right)

2 AIMS

The specific purpose of the work is to evaluate how the WEPTOS performance is affected by the presence of a spring into the system that applies a torque inversely proportional to the degree of rotation of the rotors. The "negative" spring induce a large torque on the rotor in presence of small deviations from the equilibrium conditions (in calm waters), so that rotations are enhanced. As the rotation increases, the torque decreases.

3 PHYSICAL MODEL TETST

The tests were carried out in the deepwater wave basin of Aalborg University, having dimensions 15.7 m x 8.5 m x 1.5 m. Water depth in the testing area was constant, equal to 0.7 m. Opposite the wave-generator an artificial beach made of stones was used to reduce wave reflection. Five wave gauges measured the surface elevation.

The physical model of a single rotor in scale 1:29.4 is tested in two different versions: with and without a negative spring inserted into the mechanism. The aim of the tank tests is to evaluate the effects of the negative springs in terms of power production inserted in the model.

The rotor is essentially a drum of fiber-glass filled with foam. It has a width of 0.24 m, a chord of 0.326 m and a diameter around the axle of rotation of 0.21 m. The weight of the body of the single rotor is 4.083 kg. The angle at rest is 45°. The rotor during the tests was clumped to an upper bridge, which crosses the entire basin along the shorter side, but was free to float in the vertical direction.

Two different springs are used to test the influence of the negative stiffness: the first spring (k1) has a stiffness of 1876.5 N/m and it is 117 mm long at rest. The second spring uncompressed (k2) is 127 mm long and has a stiffness of 946.53 N/m.

The PTO system was simulated through the friction of a pre-tensioned cable around a metallic wheel free to rotate around its axle, to guarantee the best ‘gear’ in the production of the mechanical power.

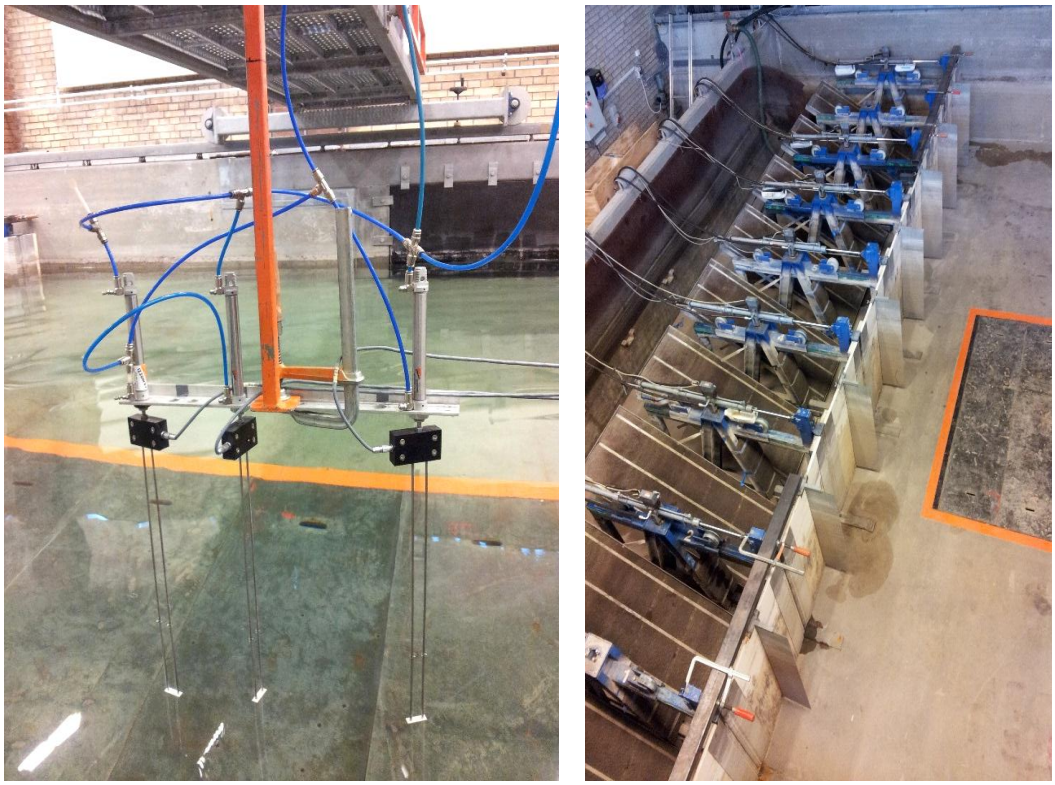

Figure 2: Wave gauges (left) ; Wave maker (right)

The difference between the forces on the cable due to the incoming waves is measured by two force transducers located at the extremities of the strip used to apply the pretension force.

The performance of the system is expressed through the non-dimensional performance (ND), i.e. the ratio between the power absorbed by the device and the available wave power for specific wave conditions. The whole quantity is theoretically independent of the scaling ratio of the device, but is in practice affected by several model and scale effects.

Figure 3: Rotor (left) ; potentiometer (right)

3.1 Structure eigenfrequencies

The natural oscillations of the structure are related to the structure mass and stiffness, the damping of the free oscillation is related to the energy dissipation terms.

Table 1: Results of free oscillation analysis

	NO SPRING	K2	K1
Logarithmic decrement	0.827	0.514	0.458
Damping ratio	0.130	0.081	0.072
Damped frequency [1/s]	1.021	0.760	0.678
Natural frequency [1/s]	1.030	0.763	0.679
Natural period of oscillation [s]	0.970	1.310	1.470

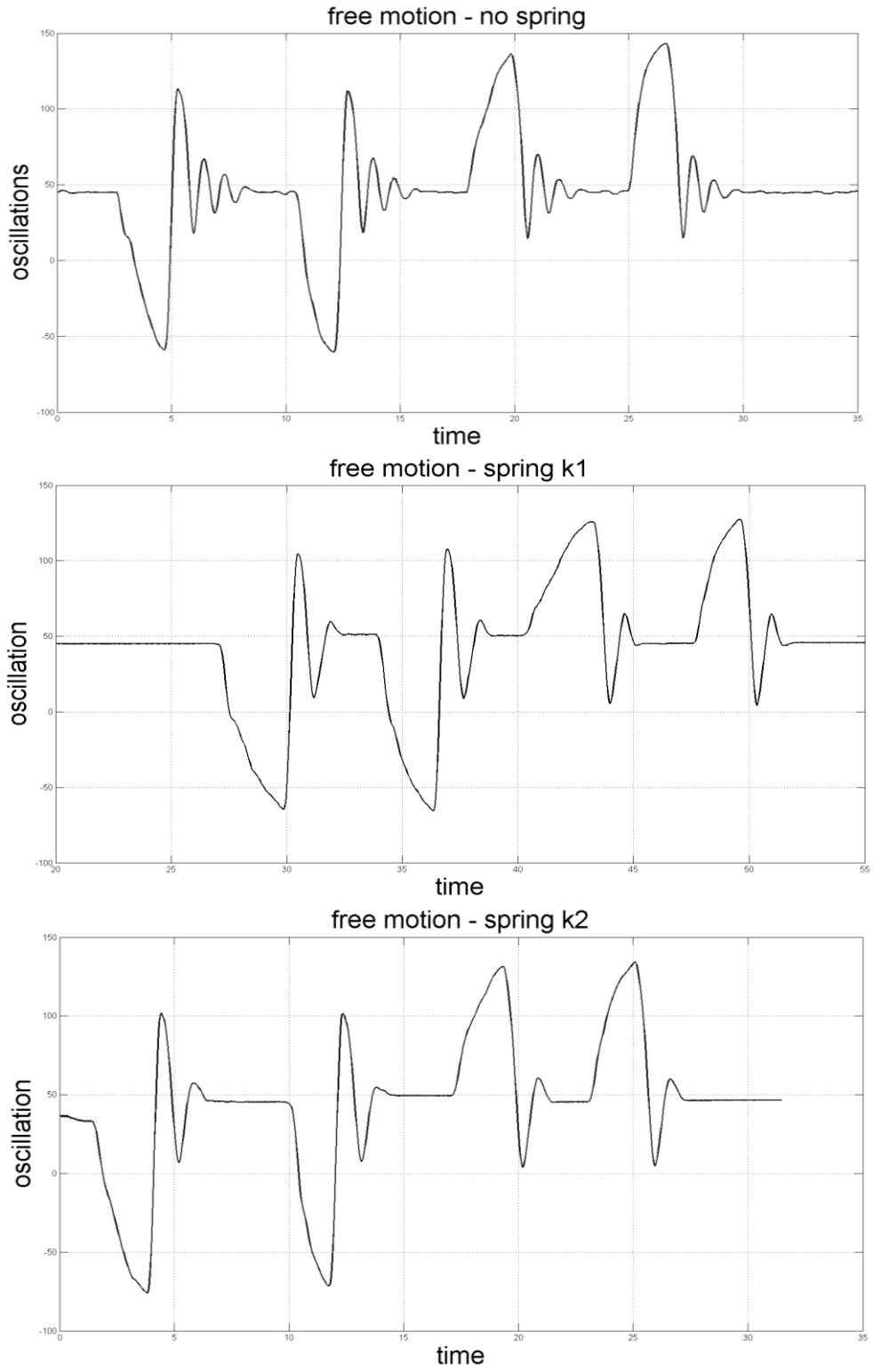

Figure 4: Record of free oscillations (4 tests)

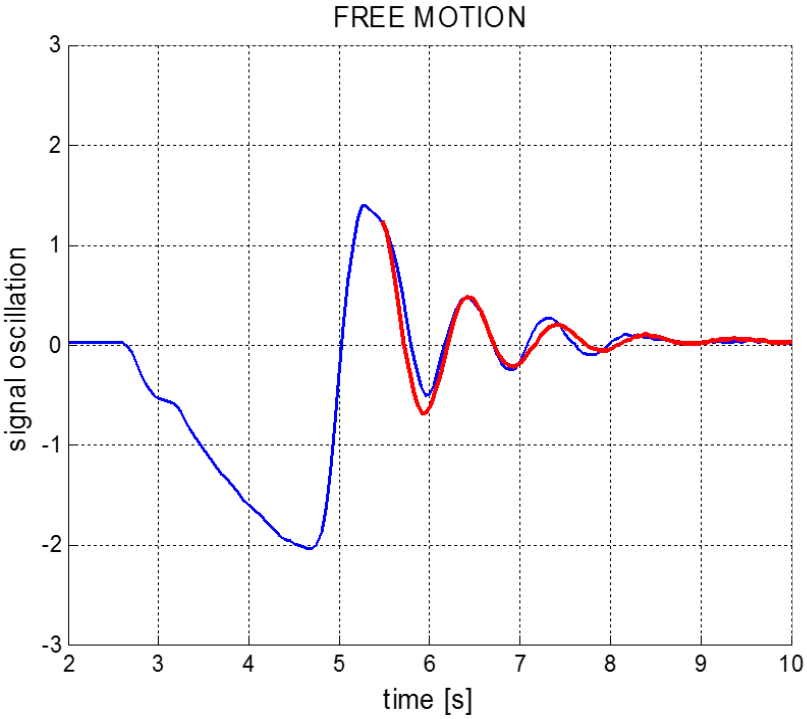

Figure 5: Free motion interpretation

The free motions are analysed by displacing the rotor in water, i.e by rotating it until it appeared well out of equilibrium, and rapidly releasing it 4 times (in the 2 opposite directions), in presence and in absence of the (negative) springs. The measured oscillations (Figure 4) of the rotor were analysed (Figure 5) to find the frequency and the damping characteristics (Table 1).

Fig 4 shows that a much lower damping (larger oscillations) is found in absence of the springs. In fact the springs also induce a very large friction, which is clearly a model effect.

Adding the negative spring k1 the natural period of oscillation increases from 0.979 to 1.325 s, and with the negative spring k2 the natural period becomes 1.4708 s. In conclusion the value of the natural frequency decreases with the 'negative' spring: the decrease is larger with the second spring than with the first one.

3.2 Test Programme

First, regular waves were used to analyse the hydrodynamic behaviour of the device under different wave conditions. Every batch takes 1 minute, where the wave height is constant (equal to 0.06 m) and the wave period is incremented at each step. The periods used are: 0.7, 0.8, 0.85, 0.9, 0.95, 1, 1.05, 1.1, 1.15, 1.2, 1.3, 1.4, 1.5, 1.65, 1.8, 2 seconds. During these tests the rotor can move freely and the oscillation of the device is recorded by the potentiometer.

Then, irregular waves were used to analyse the performance of the rotor under irregular wave conditions, in terms of power production, and the PTO mentioned previously is inserted in the system. Five sea states (Table 2) which represent the Danish part of the North Sea have

been analysed (water depth of 18 m):

Table 2: Generated wave and associated incident wave power (prototype and scale)

WS	Prototype scale			Model scale		
	Hm0	Tp	Pwave	Hm0	Tp	Pwave
	[m]	[s]	[kW]	[m]	[s]	[kW]
1	1.01	5.4	2.46	0.034	0.998	0.51
2	1.39	6.2	5.32	0.047	1.148	1.12
3	1.92	7	11.41	0.065	1.296	2.43
4	2.55	7.8	22.67	0.087	1.448	4.85
5	3.15	8.7	38.04	0.107	1.597	8.10

These states are recreated into the laboratory (water depth of 0.61 m; JONSWAP with γ 3.3). According to the scale ratio chosen (1:29.4) the values are the following:

The sea states that are analysed in greater detail are WS3 and WS4.

4 TEST RESULTS

4.1 Oscillations without PTO (regular wave)

The best response in terms of oscillation of the system is reached when the period of the waves is more or less equal to the period of natural oscillation of the system (T_n), which is different for every configuration.

For the system without any springs Tn = 0.97 s. It means that for regular wave state with H= 0.06 m and T= 1.0 s the system is not so far from the conditions of resonance. The resonance is Tn= 1.31 s and 1.47 s for springs k2 and k1, respectively.

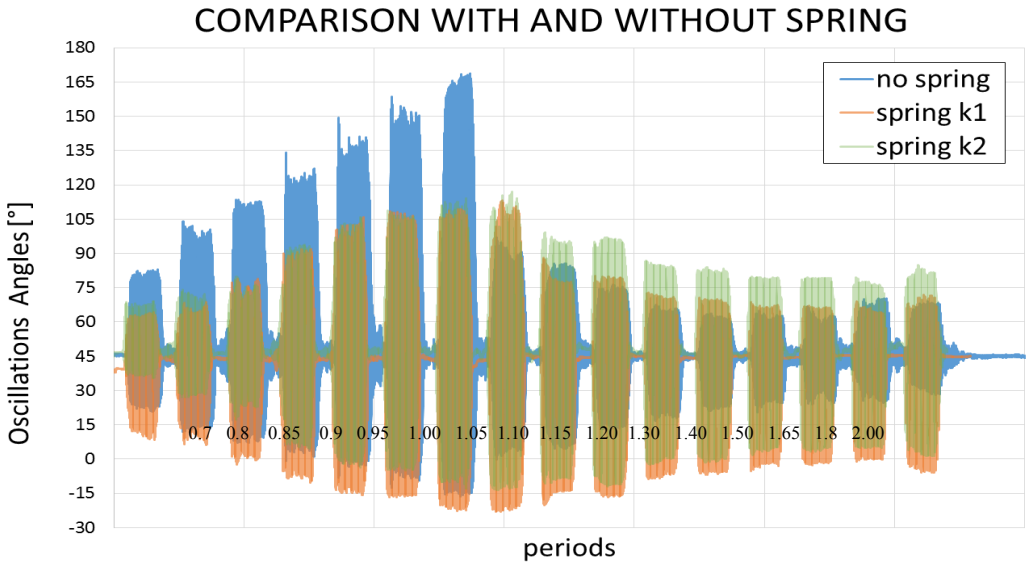

Figure 6: Record of free oscillations (4 tests)

Fig. 6 shows that the amplitude of the oscillation is maximum for the resonance period and drops for larger periods in the absence of the negative spring. The same resonant behaviour is not evident in presence of the springs, due to the large damping. However, for periods larger than 1.5 s, the oscillation is larger for the cases with a spring. Consequently, an improvement in terms of efficiency is expected for higher periods. The negative oscillation (i.e. when the rotor tip gets out of water) was larger than the positive, and in general the movement was less symmetric for the highest periods in presence of the springs.

4.2 Oscillations with PTO (irregular waves)

WS3 and WS4 are the more energetic sea states, considering the combination of probability of occurrence and incident power. Clearly, the aim is to develop the converter at its best efficiency for this sea state.

Table 3 shows the resulting non-dimensional performance in these conditions. Contrarily from expectations, the experimental results show that the performance is lower in presence of the larger negative stiffness k1. In presence of the (smaller) spring k2, results are only slightly better than without the spring.

Table 3: Experimental non-dimensional performance

CONFIG.	ND (WS3)	ND (WS4)
Without spring	0.19614	0.12956
With spring k1	0.13815	0.10806
With spring k2	0.19402	0.14247

The results can be explained because the spring caused large dissipations that masked the real performance of the rotor.

In a mechanical system the structural damping given by the friction has large influence on its operating behaviour. There are different types of damping, and part is due to the presence of the spring. Its contribution can be determined by the added damping measured during the free oscillation tests.

From the measurements done to evaluate the dissipation, it is possible to notice that the presence of the spring causes an increase of the energy dissipated for specific positions of the rotor: between 10° and 90° from the horizontal. These angles are also measured experimentally by looking at the exact moment at which the spring starts and ends to be compressed. This is the real range in which the spring works.

5 NUMERICAL MODEL

To simulate the results of the experiments, a numerical model is developed.

The system, as said previously, can be schematized as a mass-spring-damper system, forced by the oscillations of the waves. The equation which describes the system is:

$$\ddot{x} * I + \dot{x} * R + x * S = g(t)$$

Where: R is the damping factor of the system; S is the global stiffness of the system (the buoyancy K “plus” the negative spring); I is the term which describes the inertia of the

system.

The geometry of the single rotor is reproduced graphically, and the model is calibrated numerically: the quantities which describe the behaviour of the system are evaluated step by step.

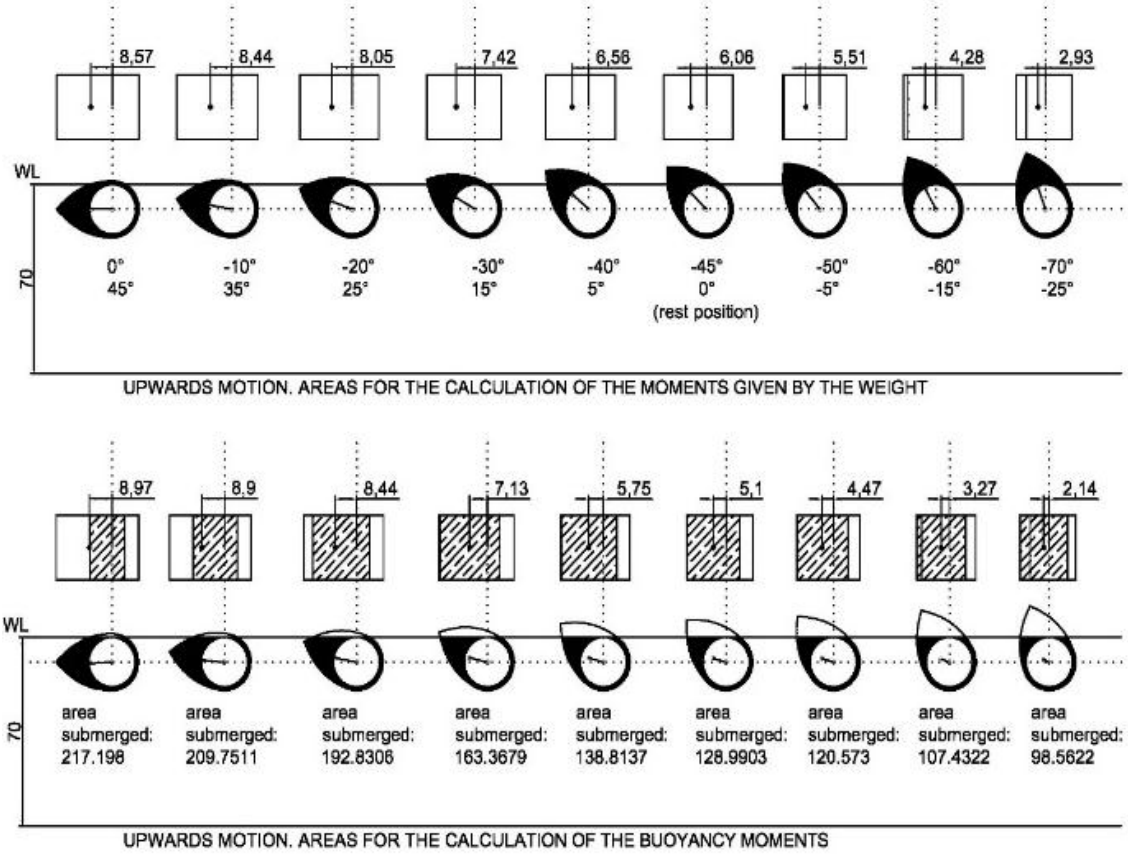

Figure 7: Graphic reproduction of the model

5.1 Calibration of stiffness

At first the total stiffness of the system is computed by reproducing numerically the trend of the hydrostatic moments of the buoy (which are estimated as the difference between the moments given by the weight and by the buoyancy).

The value of the "stiffness due to buoyancy" K is not constant and changes with respect to the relation between moments and angles. It means that, contrary to the trend of the stiffness of a simple spring, for example, the relation between the moments and the angles is not constant. In order to describe in a schematic way the behaviour of the system in terms of oscillation, it is necessary to choose one single value of K to have a specific coefficient multiplying the x to solve the previous equation.

A value of K equal to 2.2 is chosen. This corresponds to the stiffness of the system (without any spring) around the rest position, and it is also a value which expresses the average of the range.

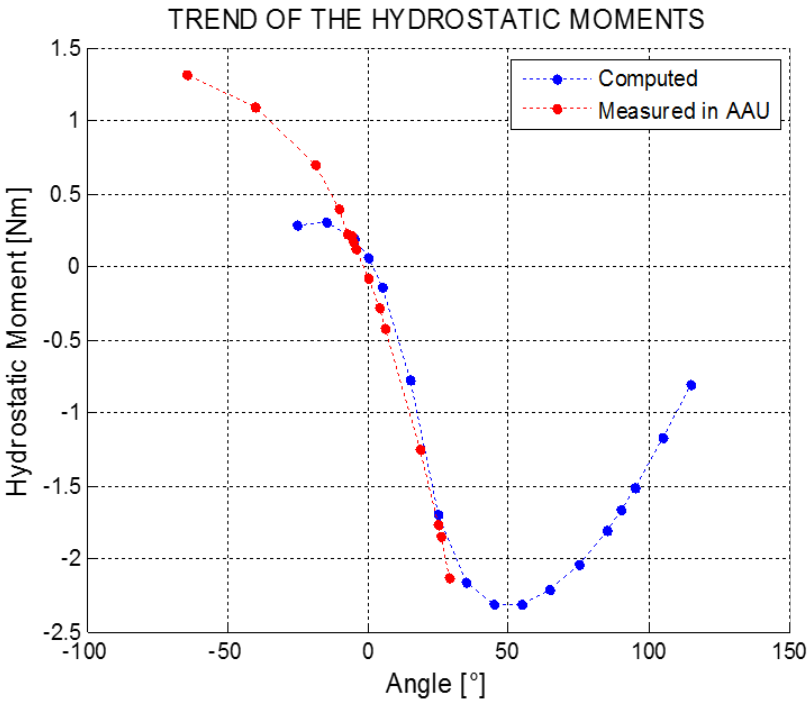

Figure 8: graphic reproduction of the model

5.2 Calibration of Inertia and of Damping coefficient

By analysing the signal of the free oscillation also the inertia and the damping coefficient are evaluated.

At the end of this 'simulation', the best values of natural period, amplitude and the damping ratio are fixed. Thanks to these characteristics, the starting values of the inertia of the system and of the damping coefficient are also estimated.

The inertia of the system is expressed by the relation:

$$I = \left(\frac{K}{w_d}\right) * (1 - z^2)$$

Where:

K is the stiffness of the system.

w_d is the damped angular frequency.

z is the damping ratio.

The damping coefficient (R/I) is given by the formula:

$$c = z * 2 * w_0 * I$$

Where:

w_0 is the natural angular frequency.

5.3 Evaluation of wave load (Transfer function)

The external force is introduced by the observation of the signal of the oscillations of the rotor when it is forced by a series of regular waves: this observation gives the experimental transfer function.

The transfer function is experimentally evaluated to have a correct superimposition between the signal measured and the one calculated. Every coefficient, that is indicative of the relation between the incident wave height and the torque due to this same wave, is a function of the wave period, and is maximum close to the natural period of oscillation of the system.

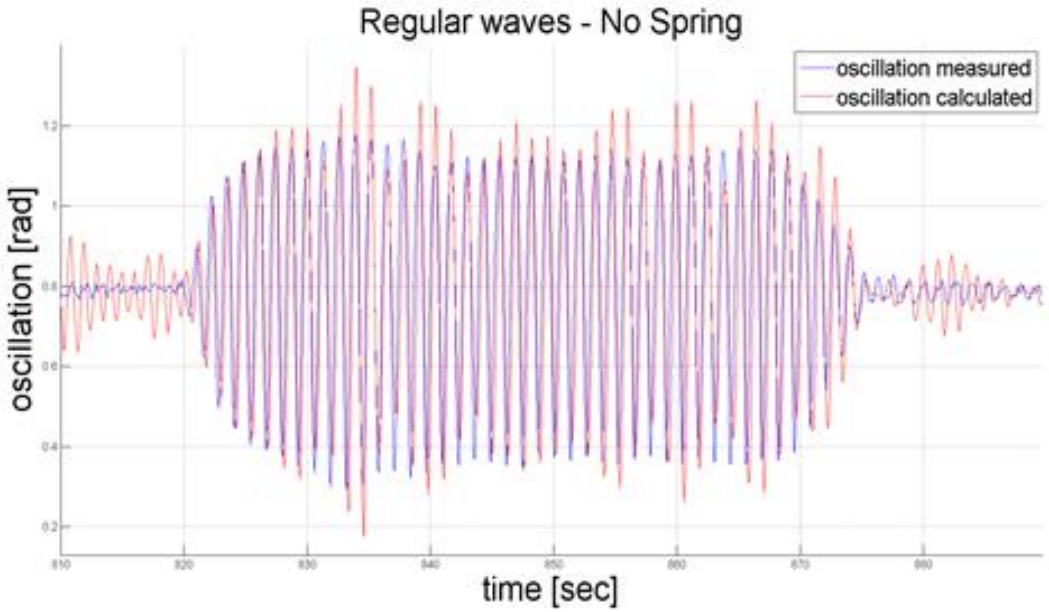

Figure 9: Result of calibration of transfer function for regular waves.

5.4 Calibration of PTO load

The term of the control force is estimated by analysing the signal of the oscillations when a load is also applied to the rotor (forced by irregular waves) to simulate the presence of a PTO system.

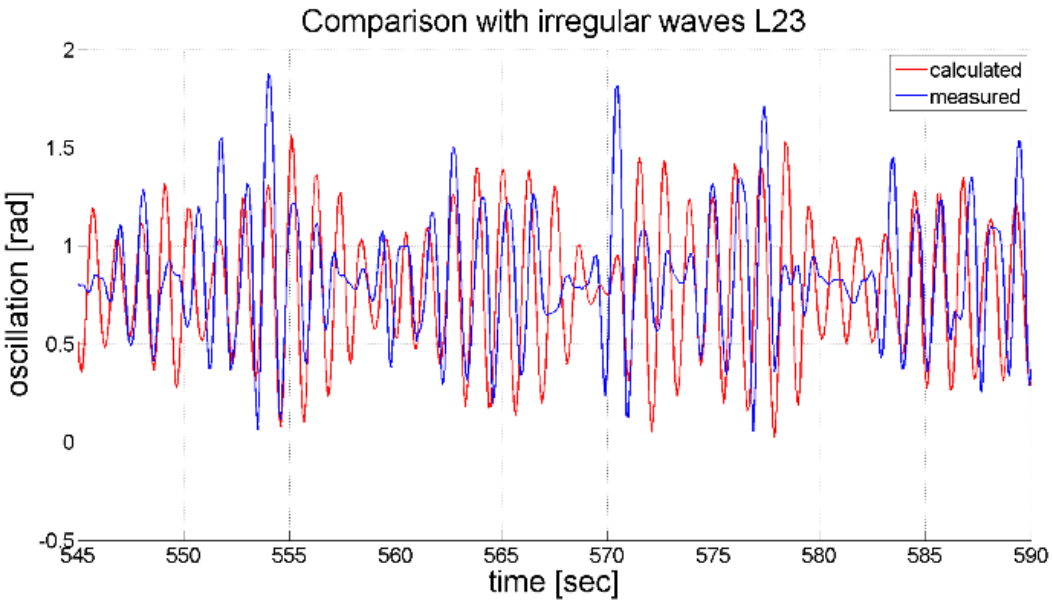

Figure 10: Result of calibtarion of PTO load based on irregular wave.

6 RE ANALYSIS WITH CALIBRATED NUMERICAL MODEL

The calibrated model is used to estimate the power related to an ideal model of the WEPTOS without the spourious friction induced by the negative springs.

The power is obtained integrating the damping force which describes the 'generator' over the angular velocity: it is the power dissipated by the damper:

$$P = \int c_{gen}\dot{x} \cdot \mathrm{d}\dot{x}$$

Where:

c_{gen} is the damping coefficient related only to the specific load applied.

$\dot{x}$ is the velocity.

P is the power dissipated by the 'generator' with a specific load applied.

c_{gen} is evaluated by the difference between the damping coefficient of the system without the PTO loads, and the one of the system with the applied PTO load. The damping in presence and in absence of load are evaluated as explained in Section 5.2. Then, the generator contribution is obtained by:

$$c_{gen} = c_{load} - c_{no\_load}$$

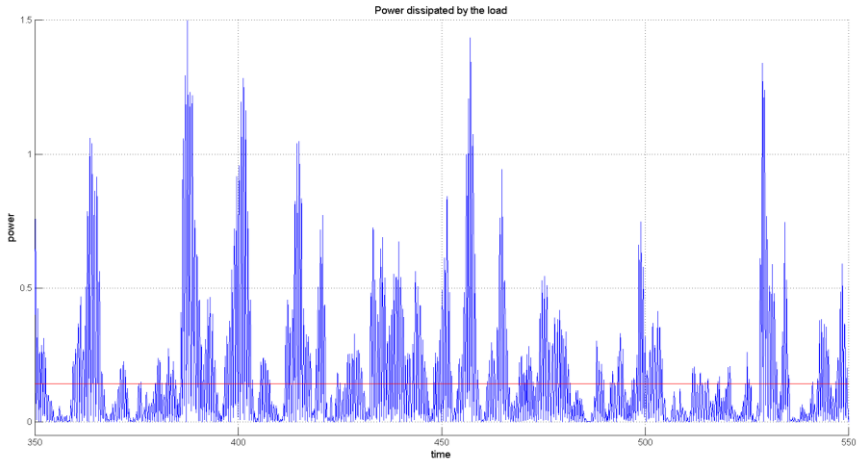

Figure 11: Simulation of power production – WS3, no spring

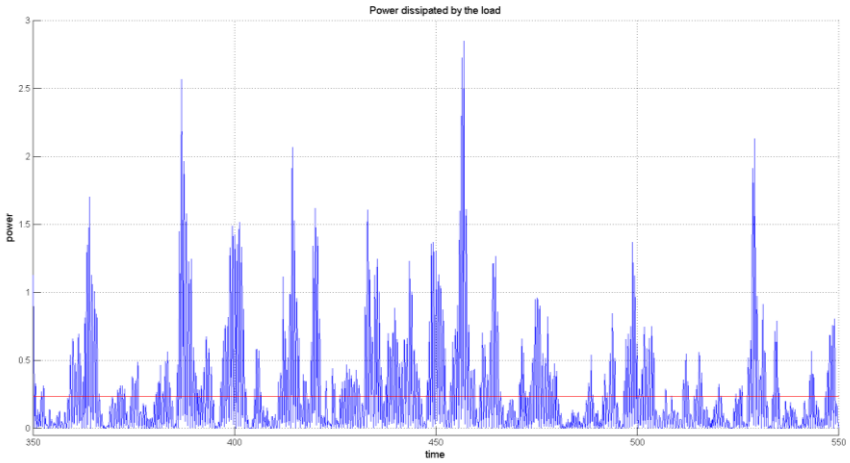

Figure 12: Simulation of power production – WS3, negative spring k1

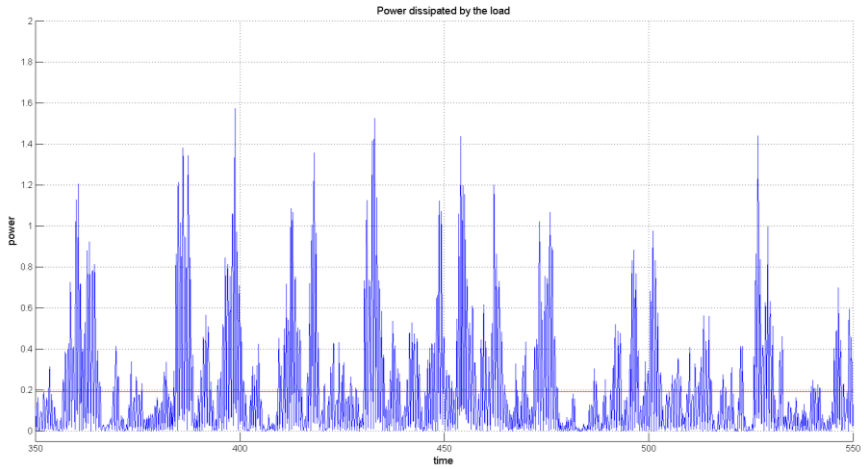

Figure 13: Simulation of power production, – WS3, negative spring k2

This approach allows to generate numerical sequences removing from the data the spurious friction induced by the negative springs. Figures 11, 12, 13 show the results of the simulation for WS3.

Figure 14 summarises the results of the simulations for WS3 and WS4, i.e. the two wave attacks that mostly contribute to the overall energy content.

From the numerical simulations, carried out in absence of the undesired friction induced by the presence of the negative springs, the non-dimensional performance is larger for the configurations with the springs.

The stiffest spring gives an higher value of the ND performance in comparison to the other configurations. The better response is clearly noticeable for the WS3, whereas is less noticeable for the WS4.

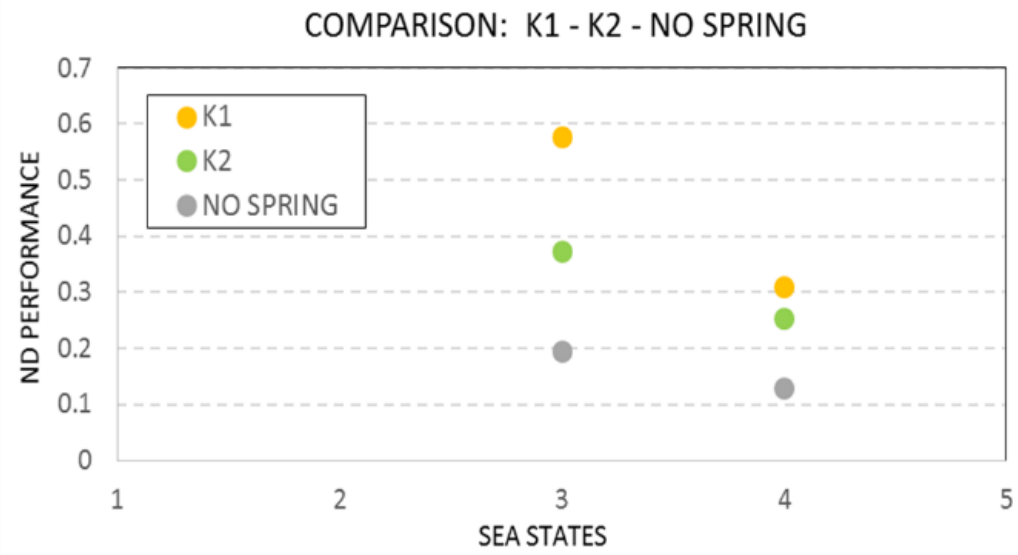

Figure 14: Simulated non-dimensional performance

7 CONCLUSIONS

Physical model tests were carried out on a single rotor of the WEPTOS device using springs that modeled 3 different negative stiffness conditions: two different springs were insalled and the behaviour of the rotor compared to the preliminary tests performed without any spring.

The experimental results appeared to show that the model with larger negative stiffness was the less efficient device for all tested waves. Even the tests with the “milder spring” did not show a real increase in the rotor performance (with respect to the WEPTOS without any negative stiffness spring). Indeed the larger spring caused large dissipations that masked the real performance of the rotor.

In order to better interpret the results, a numerical model was set-up where the rotor is a rigid body subject to waves and restrained by a dash-pot, simulating the Power Take Off, and by introducing a negative stiffness. The method used to calibrate the model is described.

Numerical results showed that an increase of performance of 60% can be expected if a negative spring is included in the rotor device design.

In conclusion, it is possible to assert that the addition of a negative stiffness mechanism is

a possible design solution to be considered in order to increase the overall performance of these types of energy converters.

REFERENCES

Azzellino, A., Contestabile, P., Ferrante, V., Lanfredi, C., & Vicinanza, D. (2011). Strategic environmental assessment to evaluate WEC projects in the perspective of the environmental cost-Benefit analysis. In Proceedings of the 21th International Conference ISOPE, Maui, Hawaii, USA, ISBN (pp. 1-880653).

Ferri, F., Bingham, H., Zanuttigh, B., Bard, J., Kramer, M., Sørensen, J. D., & Kofoed, J. P. (2014): Advance in modelling and structural design of wave energy devices, ICOE2014, 10 pp.

López, I., Andreu, J., Ceballos, S., de Alegría, I. M., & Kortabarria, I. (2013). Review of wave energy technologies and the necessary power-equipment. Renewable and Sustainable Energy Reviews, 27, 413-434.

Martinelli L, Pezzutto P. and Ruol P. (2013), *Experimentally based model to size the geometry of a new OWC device, with reference to the Mediterranean Sea wave climate*, Energies, 6(**9**), 4696-47206.

Martinelli L., B. Zanuttigh and J.P. Kofoed (2011), *Selection of design power of wave energy converters based on wave basin experiments*, Renewable Energy, Vol. 36(**11**), , 3124-3132.

Martinelli, L., Ruol, P., Fassina, E., Giuliani, F., & Delmonte, N. (2014). A wave-2-wire experimental investigation of the new "Seabreath" wave energy converter: the hydraulic response. Coastal Engineering Proceedings, 1(34), structures-29.

Pecher, A., Kofoed, J. P., Larsen, T., & Marchalot, T. (2012). Experimental study of the weptos wave energy converter. In ASME 2012 31st International Conference on Ocean, Offshore and Arctic Engineering (pp. 525-534). American Society of Mechanical Engineers.

Pecher, A., Kofoed, J. P., & Larsen, T. (2012b). Design specifications for the Hanstholm WEPTOS wave energy converter. Energies, 5(4), 1001-1017.

Salter, S.H. (1974). Wave power. Nature 1974, 249, 720–724.

Vicinanza, D., Contestabile, P., & Ferrante, V. (2013). Wave energy potential in the north-west of Sardinia (Italy). Renewable Energy, 50, 506-521.